

Article

Effect of Propeller Cup on the Reduction of Fuel Consumption in Realistic Weather Conditions

Mina Tadros ^{1,2,*} , Roberto Vettor ¹ , Manuel Ventura ¹ and C. Guedes Soares ¹ 

¹ Centre for Marine Technology and Ocean Engineering (CENTEC), Instituto Superior Técnico, Universidade de Lisboa, Av. Rovisco Pais 1, 1049-001 Lisboa, Portugal; roberto.vettor@centec.tecnico.ulisboa.pt (R.V.); manuel.ventura@centec.tecnico.ulisboa.pt (M.V.); c.guedes.soares@centec.tecnico.ulisboa.pt (C.G.S.)

² Department of Naval Architecture and Marine Engineering, Faculty of Engineering, Alexandria University, Alexandria 21544, Egypt

* Correspondence: mina.tadros@centec.tecnico.ulisboa.pt

Abstract: This paper presents the effect of a propeller cup on the propeller cavitation and the fuel consumption of a bulk carrier in both calm water and different weather conditions towards improving the energy efficiency of the ship and reducing the level of emissions in terms of design and operation. Based on the propeller optimization model, previously developed that couples NavCad and a Matlab code to select the geometry and the operating point of the propeller at the engine operating point with minimum fuel consumption, the optimized propeller performance is evaluated for different percentages of the cup; light, medium and heavy and compared with the performance of the propeller without a cup in both calm water and several sea states. By evaluating the cavitation criteria, it is concluded that increasing the percentage of cupping reduces the occurrence of cavitation based on the Keller and Burrill methods; moreover, the fuel consumption is reduced by up to 5.4% and 6.6% at the propeller with a higher percentage of cup compared with the uncapped propeller in calm water and among the ship route, respectively.

Keywords: bulk carrier; propeller cup; fuel consumption; decarbonization; weather condition; cavitation



Citation: Tadros, M.; Vettor, R.; Ventura, M.; Guedes Soares, C. Effect of Propeller Cup on the Reduction of Fuel Consumption in Realistic Weather Conditions. *J. Mar. Sci. Eng.* **2022**, *10*, 1039. <https://doi.org/10.3390/jmse10081039>

Academic Editor: Kostas Belibassakis

Received: 5 July 2022

Accepted: 27 July 2022

Published: 28 July 2022

Publisher's Note: MDPI stays neutral with regard to jurisdictional claims in published maps and institutional affiliations.



Copyright: © 2022 by the authors. Licensee MDPI, Basel, Switzerland. This article is an open access article distributed under the terms and conditions of the Creative Commons Attribution (CC BY) license (<https://creativecommons.org/licenses/by/4.0/>).

1. Introduction

The International Maritime Organization (IMO) has applied stringent regulations to reduce the amount of exhaust emissions, especially the level of greenhouse gas (GHG) in the maritime industry; these regulations aim to achieve a reduction in the carbon intensity by at least 40% by 2030 and the total annual GHG by at least 50% by 2050 compared to 2008 [1]. The level of emissions is evaluated using several types of indices, which can be applied to the new ship, such as the Energy Efficiency Design Index (EEDI). At the same time, the Energy Efficiency Existing Ship index (EEXI) and the Carbon Intensity Indicator (CII) take into account the design and operational points of view that will enter into force at the beginning of 2023 for the existing ship.

Several solutions are proposed to improve the energy efficiency of the ships, mainly consisting of reducing the amount of fuel consumption and thus, exhaust emissions as well as increasing the amount of cargo held at a suitable ship speed [2]; these solutions mainly focus on optimizing engine performance [3] to support fuel conversion techniques to replace the fossil fuel used in ship operation with new clean fuels with much fewer carbon emissions, such as biofuel, natural gas, methanol and ammonia [4–8]; moreover, installing after-treatment systems, especially the carbon capture and storage (CCS), will be an effective solution to capture the carbon emissions before entering the atmosphere [9,10]. Other solutions consider the design of the ship hull [11,12] and improving the propulsive coefficients [13,14] combined with the use of wind energy [15] and managing the ballast system [16,17], as well as finding the optimal route [18,19] and reducing speed [20–22],

which based on simulations, becomes essential to assist the shipmaster during the voyage to reduce the resistance on the hull and thus use lower energy to operate the ship; this is mainly thanks to the online availability of wind and wave weather data worldwide [23].

The propeller selection, which is the main focus of this paper, is another area of interest in reducing fuel consumption and ensuring the sustainability of the ship along the trips. Selecting the propeller at the maximum efficiency is important to ensure a high propeller performance during the design [24–26] and operation, especially in sea states [27,28] and comply with the cavitation limits. Furthermore, the vibration and noise can be reduced, and the propeller efficiency can increase by considering the propeller boss cap fins [29]; moreover, the selection of propellers by minimizing the fuel consumption is performed in Refs. [30–33], which has been extended in Ref. [34] to ensure both objectives; maximum propeller efficiency and minimum fuel consumption.

Considering the propeller cup while designing the propeller can improve the propeller performance by increasing the thrust loading and cavitation margin. A propeller cup is the deformation of a propeller's trailing edge toward the pressure face, as shown in Figure 1 acts as a propeller with a higher pitch. As a result, the pressure distribution is changed along the blade, which increases the lift force toward the trailing edge. According to MacPherson [35], the propeller cup is computed as a percentage of the propeller diameter and varies from 0.5% for the light cup to 1.5% for the heavy cup.

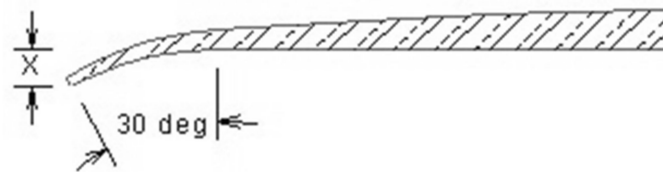


Figure 1. Section of propeller with a cup [35].

Few papers have investigated the effect of the propeller cup on the overall propeller performance. Hwang et al. [36] compared the measured data to show the effect of the cup on a series of three-blade Gawn-Burrill propellers. The value of cavitation is computed, and the cup percentage can be estimated. Tsai [37] studied the performance of a propeller with a cup, and the author showed an increase in the lift force and suggested an improvement in cavitation. Yari and Moghadam [38] used the boundary element method (BEM) to predict the performance of a partially submerged propeller (PSP) with and without a cup. The computational results are validated using experimental data; they concluded an increase in the static pressure of the face side, an increase in thrust coefficient of more than 50% and a decrease in torque coefficient with the same percentage as the thrust coefficient among all advance coefficients. Samsul [39] used the computational fluid dynamics (CFD) method to study the effect of a propeller cup on cavitation. The author achieved lower cavitation in the case of the propeller cup than in the uncupped propeller.

From that point of view, the contribution of this paper focuses on presenting the effect of propeller cupping in terms of fuel consumption toward ship decarbonization and the assessment of cavitation on propeller blades for different sea states during the trip of a bulk carrier from Europe to the USA.

The remainder of this paper is organized as follows. The numerical model used to perform the simulation is presented in Section 2. The computed results and the evaluation of the propeller performance in both calm water and weather conditions are presented in Section 3. Finally, a summary of the main findings and future recommendations are presented in Section 4.

2. Numerical Model

The numerical model that is used to perform the simulation in this study is a propeller optimization model that was previously developed by Tadros et al. [31], coupling NavCad software [40] and a nonlinear optimizer. The main objective of this model is to benefit from

the operation research technique to select the propeller geometry at the engine operating point with minimum fuel consumption and verify the proposed constraints. More details about the developed numerical tool that is consisted of two modules to optimize the engine and propeller performance can be found in Refs. [3,31,34,41–44].

In this study, a bulk carrier 154 m in length is chosen as a case study to perform the numerical simulation. The ship’s characteristics and the main engine installed are given in Tables 1 and 2, respectively.

Table 1. Main characteristics of the bulk carrier.

Item	Unit	Value
Length waterline	m	154.00
Breadth	m	23.11
Draft	m	10.00
Displacement	tonne	27,690
Service speed	knot	14.5
Maximum speed	knot	16.0
Number of propellers	-	1
Type of propellers	-	FPP
Rated power	kW	7140

Table 2. Main characteristics of diesel engine [45].

Item	Unit	Value
Engine builder	-	MAN Energy Solutions
Brand name	-	MAN
Bore	mm	320
Stroke	mm	440
Displacement	liter	4954
Number of cylinders	-	14
Rated speed	rpm	750
Rated power	kW	7140

Once the ship is chosen, a systematic procedure is applied to define all the inputs required in NavCad as described in Ref. [31] to select the propeller geometry and the operating point based on the gearbox ratio at the design speed. The computed parameters are exported from Maxsurf [46] based on the defined 3D hull of the ship and then defined in NavCad. A range of ship speeds, the series of the propeller (Wageningen B-series [47]) and the number of blades (five blades), the engine load diagram and the efficiencies of the propulsion system are introduced. After filling all the required inputs, the Holtrop method is presented in Refs. [48,49] is selected to compute the ship resistance associated with the speed range, while the method presented in Holtrop and Mennen [50] is considered for computing the propulsive coefficients such as wake fraction, thrust deduction factor and relative rotative efficiency and these methods show a good agreement with CFD results [51].

Other methods can be used during the resistance and propulsion computation and integrated into the software, while these two selected methods are ranked first based on the expert ranking provided in NavCad. Due to the uncertainty of these methods, as they are based on regression models and require validation with real tests or CFD models [51], a design margin of 10% is considered during the computation of ship resistance. The same procedures are considered by changing the value of the propeller cup from light to medium to heavy presented in mm, and as a function of propeller diameter as in the following equation:

$$Prop_{Cup-mm} = Prop_{Cup-percentage} \times Prop_{Dia-mm} \tag{1}$$

Then, the effective propeller pitch is computed using the following expression as presented by MacPherson [35]:

$$P_{Eff} = P_{Geo} + 21(Prop_{Cup-mm}) \tag{2}$$

where P_{Eff} is the effective pitch and P_{Geo} is the uncupped face pitch.

Once the propeller characteristics are computed from NavCad, the propeller performance is integrated into the engine load diagram, previously developed in Refs. [3,52], as functions of engine speed and brake power to compute the brake-specific fuel consumption (BSFC) and the exhaust emissions.

After that, the propeller is optimized, and the performance of the system is recalculated. Figure 2 shows the schematic diagram of the optimization model to select the propeller in calm water.

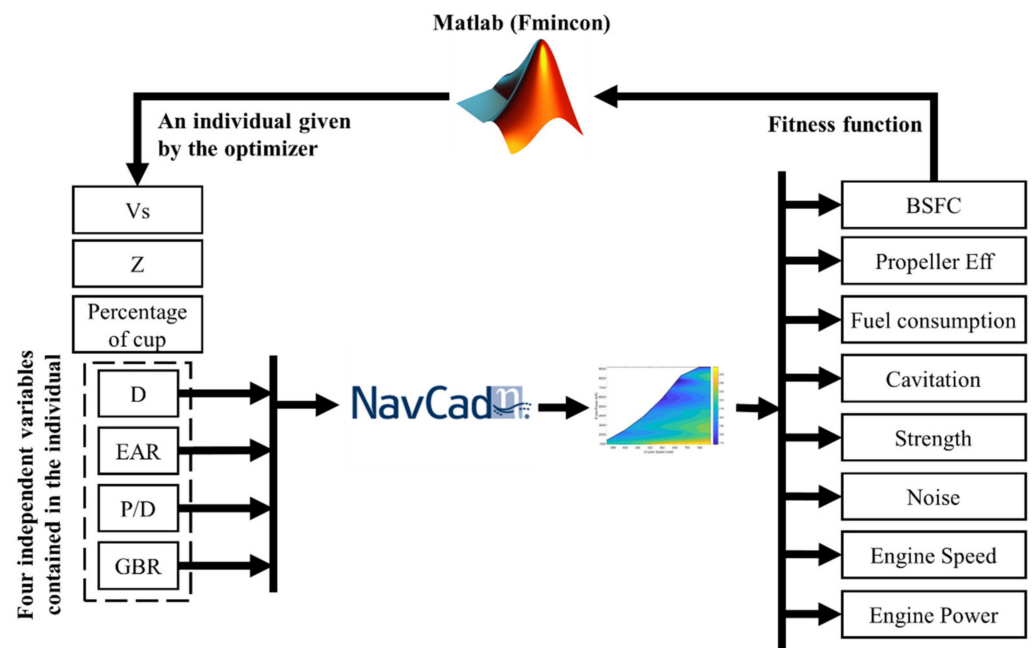


Figure 2. Schematic diagram of the propeller optimization model.

The objective and the constraints of the optimization model are combined into a developed fitness function as in the following equation, where the main objective is the minimization of fuel consumption and the constraints are related to cavitation, noise and strength issues.

$$Fitness\ Function = FC + R \sum_{i=1}^j \max(g_i(x), 0) \tag{3}$$

where FC is the fuel consumption, $g(x)$ is the static penalty function, x is the number of variables, j is the number of constraints, and R is a penalty function.

After that, the fitness function is evaluated by the nonlinear optimizer (fmincon) integrated into Matlab [53]. Although the fmincon is considered a local optimizer, several initial starts have been performed to ensure the accuracy of the results and achieve the minimum value of fuel consumption along all the trials performed.

After selecting the optimal propeller geometry and the operational point in calm water, the performance of the ship, engine and propeller are computed along the shipping route with different sea states. The considered sea states represent the expected wave climate in the northern route from the British Channel to the west coast of the US [54], as shown in Figure 3; it also accounts for the effect of storm avoidance on the probability distribution of rough weather conditions [55], where the significant wave height (H_W) varies between

0 and 10 m, and the modal wave period (T_p) varies between 4 and 18 s; moreover, the most occurrent sea state varies between 1 to 2 m and 6 to 8 s. The scatter diagram of the selected route is shown Figure 4.

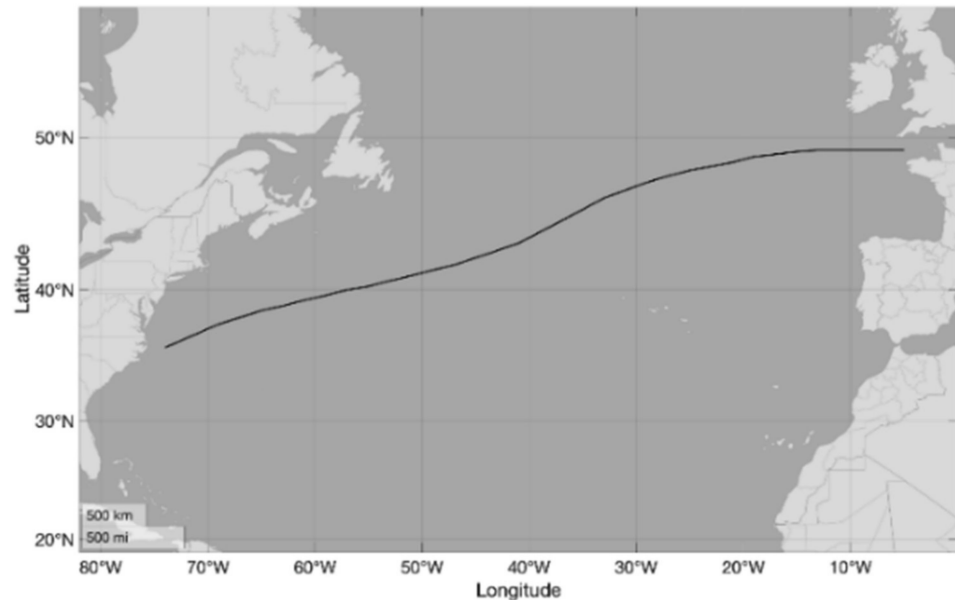


Figure 3. Northern route from the British Channel to the west coast of the US.

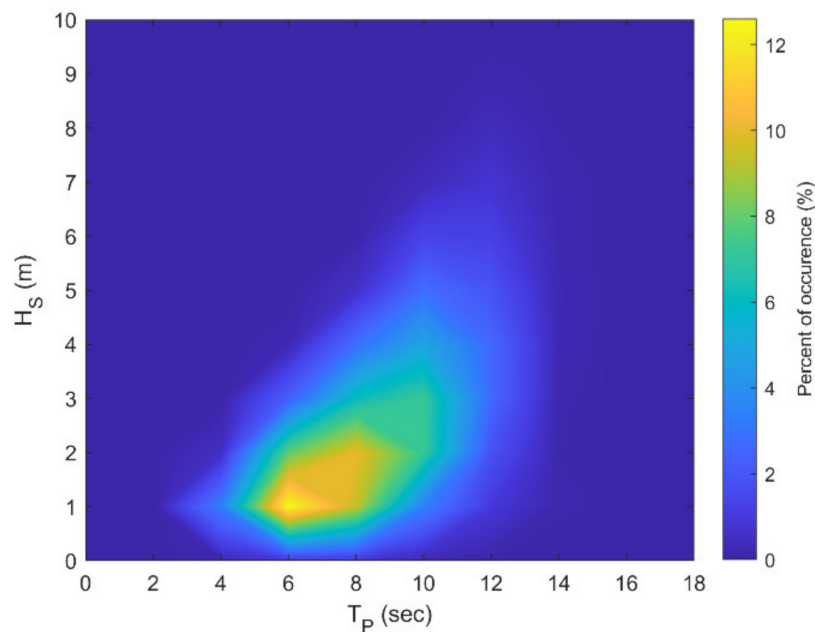


Figure 4. Scatter diagram of the northern route from the British Channel to the west coast of the USA.

Based on the collected weather data, the added resistance due to the existing waves in each sea state is computed using Aertssen [56] method; this method is integrated into NavCad, does not account for ship type and can be easily used by defining the significant wave height and modal wave period of each sea state; it is adapted by the team of HydroComp [40] to compute the added resistance due to the waves only while extracting the wind resistance.

Using an application programming interface (API), which can allow the connection between NavCad and Matlab as a third party, the simulation of all sea states is performed in a simple loop; then, the computed results are easily exported. A schematic diagram of

all the simulation and optimization processes is presented in Figure 5. For a meaningful comparison among the different configurations, the different parameters are computed for each defined sea state and then averaged, considering each weather condition occurrence using the following expression:

$$P_W = \frac{\sum_{i=1}^n P_i \times SS_{Occ,i}}{\sum_{i=1}^n SS_{Occ,i}} \quad (4)$$

where P_W is the weighted average parameter, P is the computed parameter, SS_{Occ} is the occurrence of the sea state.

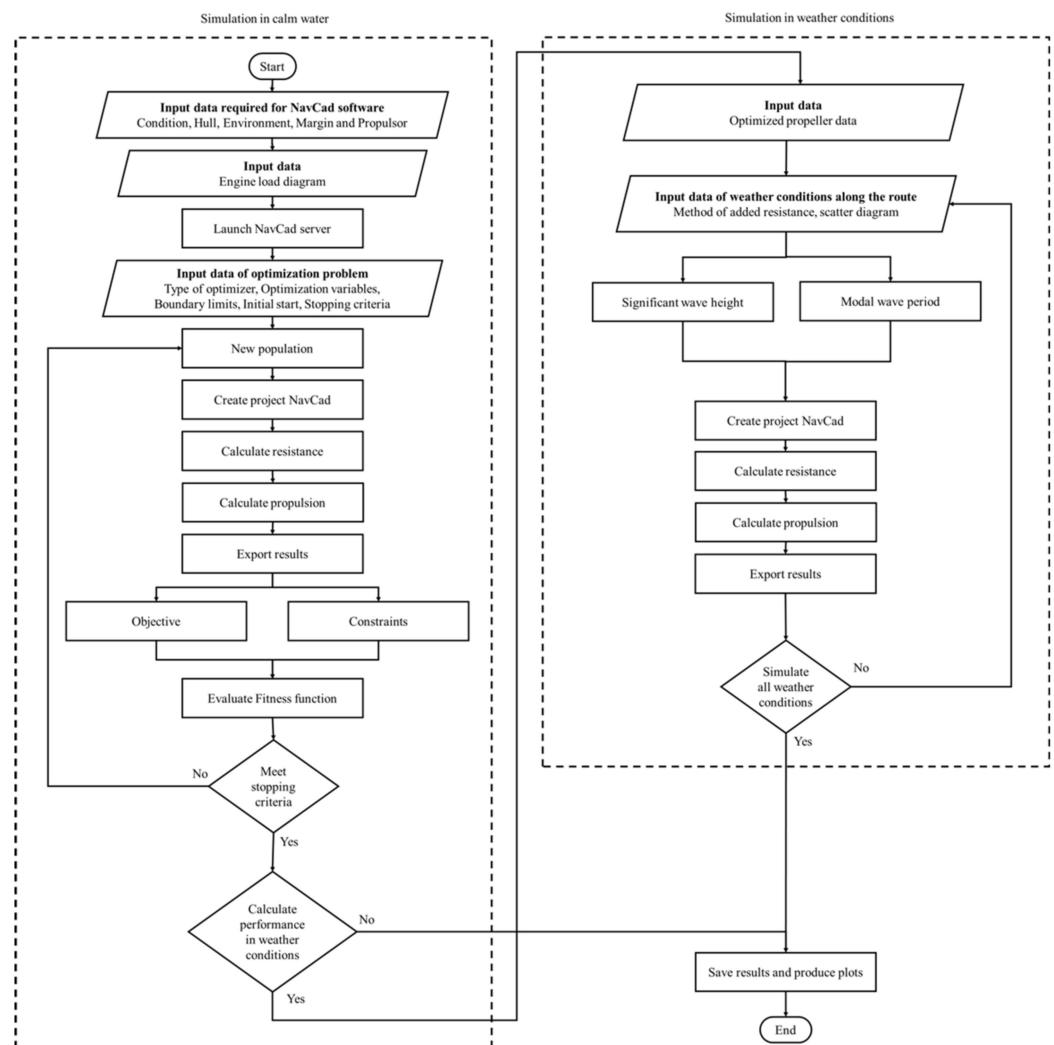


Figure 5. Schematic diagram of optimization tool in calm water and weather conditions.

3. Results

3.1. Simulation in Calm Water

First, the simulation is performed to select the optimum propeller by minimizing the fuel consumed at the design speed and in calm water conditions for several percentages of cupping, which varies from no cup to heavy cup. Table 3 shows the performance of the optimum propeller for each simulated case and the expanded view of the propeller blade is shown in Figure 6, showing the propeller cupping at the trailing edge along the four simulated cases. The propeller geometry is selected, including propeller diameter (D),

expanded area ratio (*EAR*), pitch diameter ratio (*P/D*) and the operating point computed by the relation between propeller speed (*N*) and gearbox ratio (*GBR*).

Table 3. Propeller characteristics for different percentages of cupping.

	Parameters	Unit	No Cup	Light Cup	Medium Cup	Heavy Cup
Propeller Type		Wageningen B-Series				
Ship Speed	V_s	[kn]	14.5	14.5	14.5	14.5
Propeller characteristics	Cup	[%]	0.0	0.5	1.0	1.5
	D	[m]	6.00	6.00	6.00	6.00
	EAR	[-]	0.47	0.78	0.81	0.45
	P	[m]	6.58	6.38	6.26	5.59
	N	[RPM]	75	71	68	68
	Thrust	[kN]	576.49	576.49	576.49	576.49
	Torque	[kN.m]	573.30	600.90	620.70	613.2
	η_o	[%]	0.59	0.60	0.61	0.61
	J	[-]	0.62	0.65	0.68	0.68
	K_T	[-]	0.28	0.31	0.34	0.33
	K_Q	[-]	0.05	0.05	0.06	0.06
w	[-]	0.38	0.38	0.38	0.38	
t	[-]	0.19	0.19	0.19	0.19	
Cavitation	Tip Speed	[m/s]	23.61	22.37	21.32	21.48
	EAR_{min}	[-]	0.47	0.42	0.38	0.34
	Average loading pressure	[kPa]	43.56	21.15	16.40	23.21
	Back Cavitation	[%]	7.40	2.00	2.00	2.00
	$Pitch_{min}$	[m]	4.97	5.25	5.51	5.47
Gearbox characteristics	GBR	[-]	9.50	9.63	10.06	9.88
Engine characteristics	Speed	[RPM]	714	687	682	676
	Brake Power	[kW]	4682.30	4735.80	4671.00	4552.20
	Loading ratio	[%]	65.6	66.3	65.4	63.8
	BSFC	[g/kW.h]	192	189	188	187
	Fuel consumption	[l/nm]	74.17	73.94	72.47	70.20
Exhaust emissions	CO_2	[g/kW.h]	607.99	599.27	595.47	591.98
	NO_x	[g/kW.h]	6.68	7.40	7.31	6.95
	SO_x	[g/kW.h]	9.59	9.45	9.39	9.34

The propeller is always selected at the maximum propeller diameter (6 m). At the same time, the other parameters are changed to provide a suitable thrust, which is equal among the cases and complies with the cavitation limits; it has been found that the EAR is minimized in the case of a no- and heavy-cup propeller compared to the other propellers that have a percentage of cupping. The propeller speed among the cases is almost close; it has been found among the four cases that the propeller pitch decreases when increases the cupping percentage and reaches its lowest value at the heavy cup.

Therefore, the tip speed has been reduced by up to 2.3 m/s (10%) for the cupped propeller than the normal one. The minimum area required to avoid cavitation, as suggested by Keller [57], is minimized while increasing the cupping percentage by up to 27%, reducing cavitation occurrence in different weather conditions; moreover, the value of average loading pressure suggested by Burrill and Emerson [58] is reduced while increasing the cupping percentage by up to 62.4% compared to the uncupped propeller. The back cavitation shows its lowest value among all cases compared to the limit value suggested by HydroComp [40]; moreover, face cavitation is considered by identifying the minimum value of pitch to avoid this type of cavitation, as presented in Ref. [59]; it has been found that the design pitch values are higher than the minimum required to avoid face cavitation.

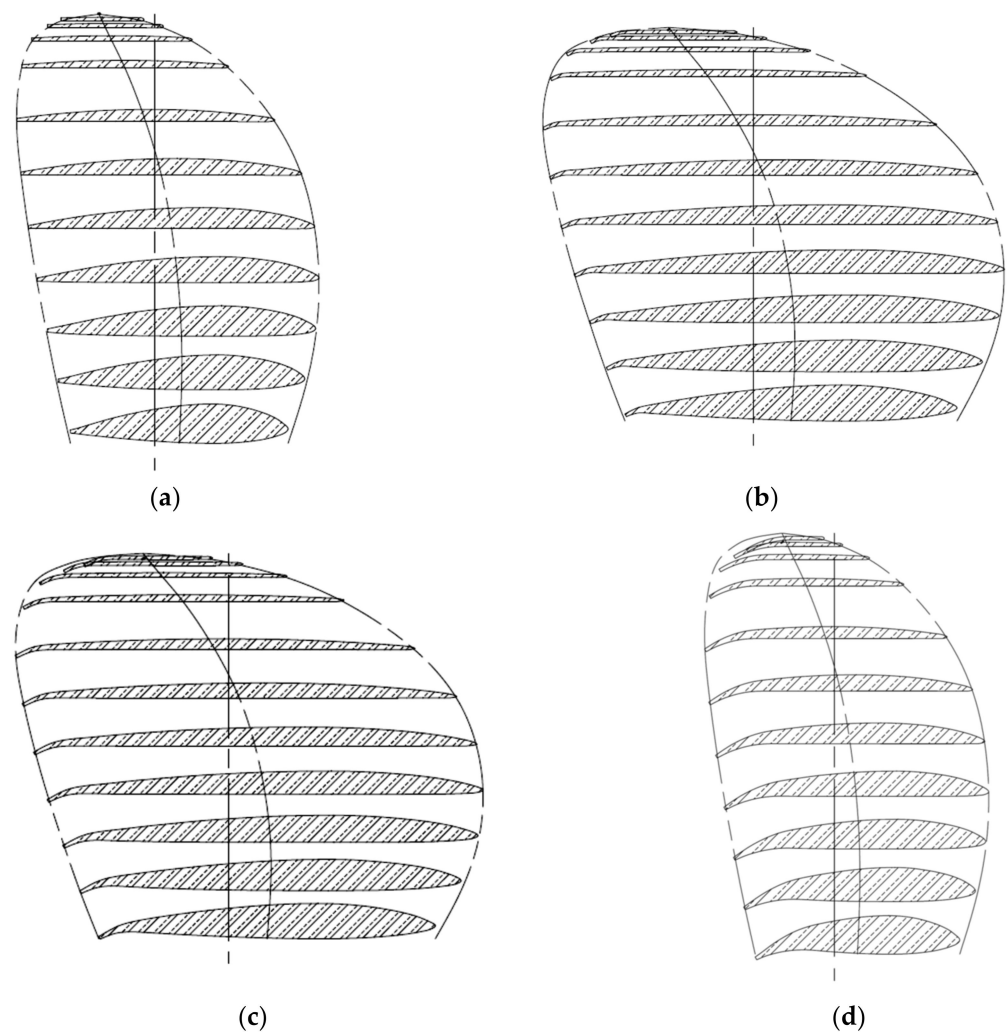


Figure 6. Expanded view of the optimized propeller. (a) No cup, (b) Light cup, (c) Medium cup, (d) Heavy cup.

Regarding the engine operating point, the propeller is selected to operate at the minimum loading conditions, which shows its lowest level at the higher cupping propeller with a reduction of 2.1% than the uncupped propeller; this achieves a reduction in fuel consumption by around 0.4%, 2.3% and 5.4% at the propeller with a light, medium and heavy cup, respectively, compared to the uncupped propeller, thus reducing the amount of exhaust emissions produced from the engine, namely the CO_2 and SO_x emissions, which has been computed based on emission factors and from the polynomial equations presented in Ref. [52].

3.2. Simulation in Different Weather Conditions

After the propeller is selected using the developed optimization model in calm water, the propeller's performance is simulated for several sea states among a selected ship route. The added resistance for each sea state is computed based on the significant wave height and modal wave period, which is then added to the calm water resistance to compute the total resistance of the ship. After that, the thrust required is computed as well as the power needed to drive the ship. Finally, the propulsive coefficients presented by the wake fraction and the thrust deduction factor are computed using empirical formulas based on the average value, and it is kept constant in both calm water and sea state conditions.

Despite the method's limitation in estimating the variation in the values of propulsive coefficients, this method shows agreement with the concept presented in Ref. [60], which is

based on experimental tests and shows that the values of propeller coefficients fluctuate around the average value computed in calm water conditions. Thus, this method shows its suitability for estimating the propeller performance in a preliminary stage for a given operating area with a defined sea state.

After simulation of the ship and propeller performance along the ship route with several sea states, it has been found that the brake power is significantly increasing so that the ship can operate at the same design speed; this increment in the value of brake power can vary between 3% at the lower conditions of sea states and about to reach 100% at high sea states conditions, as shown in Figure 7; more of an increment in brake power is achieved when the propeller is cupped than the uncupped propeller, mainly based on the propeller’s initial design and operational point.

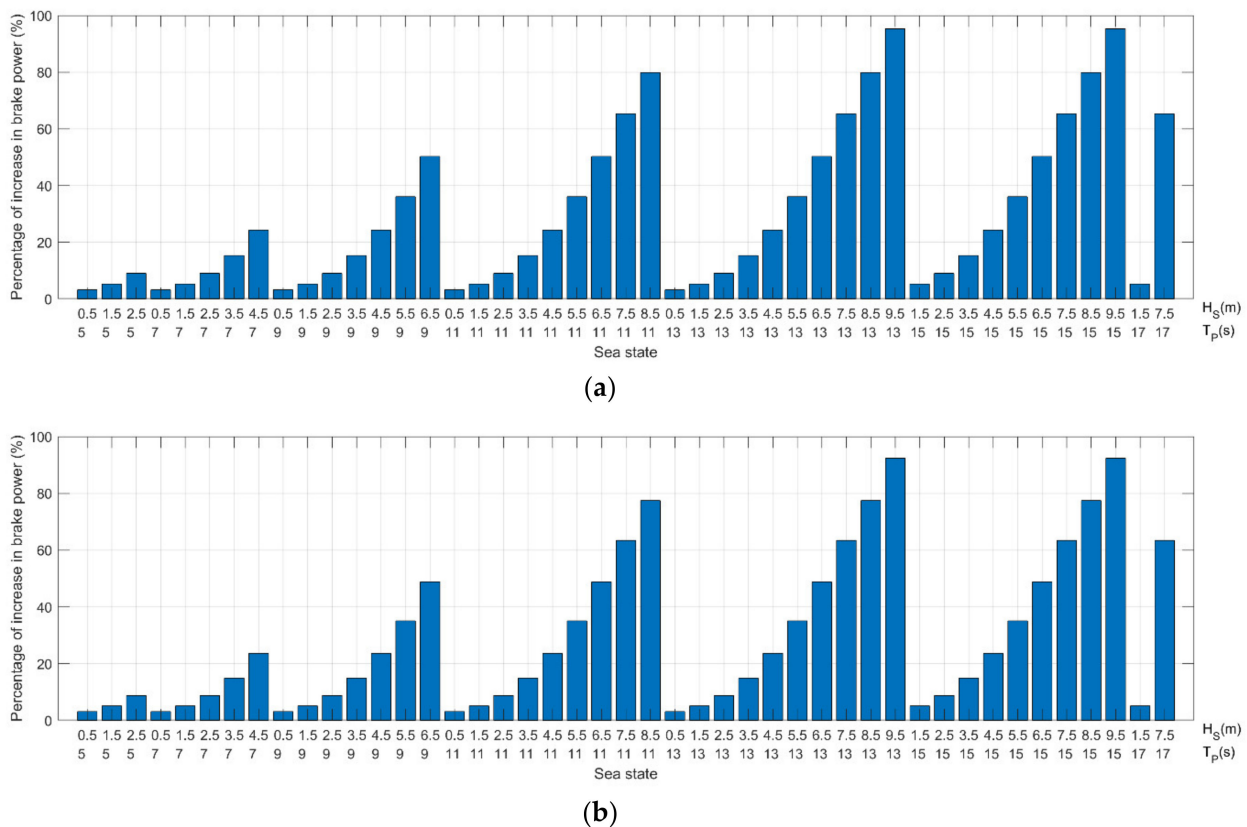
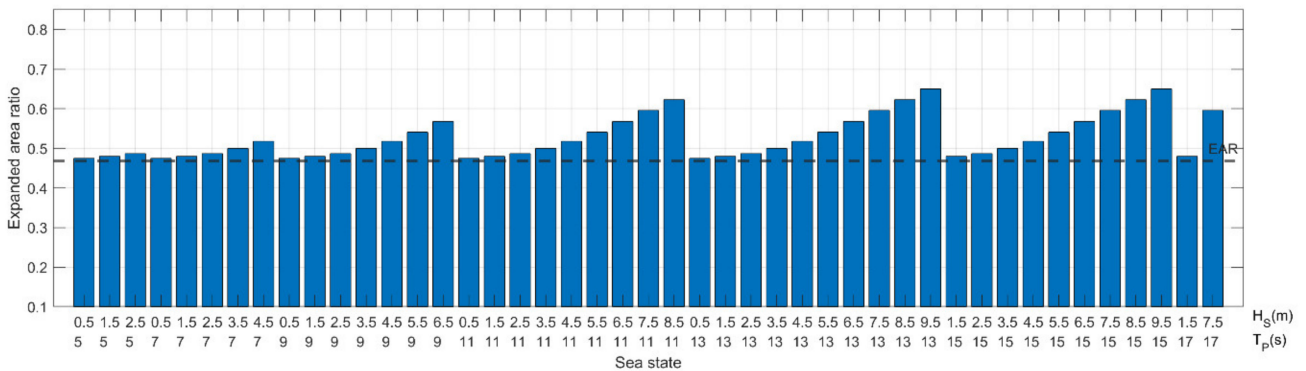


Figure 7. Percentage of increase in brake power for different sea states. (a) no cup, (b) heavy cup.

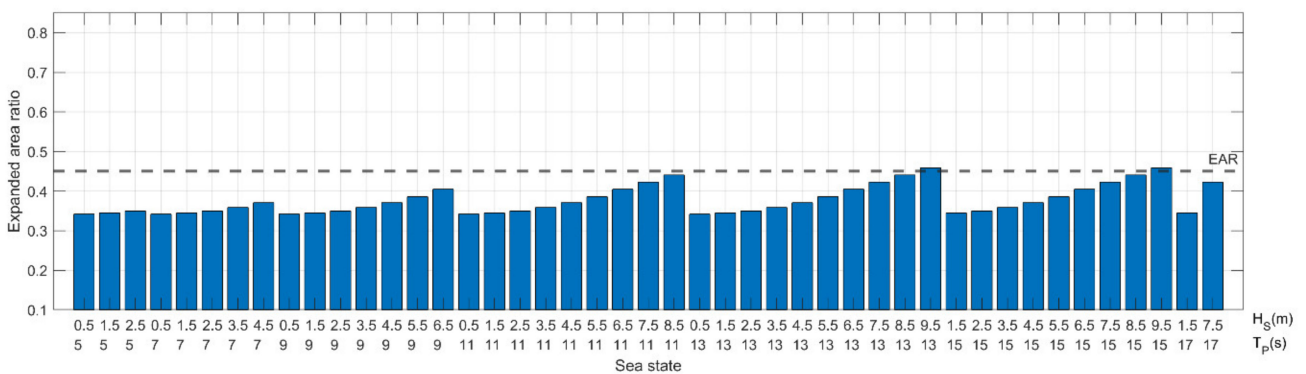
Regarding the cavitation criteria, the four techniques, as previously presented and suggested by Keller [61] and Burrill and Emerson [58] methods, are considered to quantify the limits of cavitation; these cavitation criteria are valid for calm water and under exposure to weather conditions. To consider the safety aspects during sailing in rough weather conditions, the speed reduction is limited so that the operational points of the propeller that exceed 90% of the rated power will operate at the 90% of the rated power, which is the maximum value of the continuous engine operational area.

Based on the Keller method, it has been found that the cavitation can occur in the case of the no-cup propeller in all sea states while increasing the wave height because the minimum value of EAR to avoid cavitation is equal to the designed EAR, as shown in Figure 8a. Therefore, any increase in the added resistance requires more loads, and thus the probability of occurrence of cavitation increases. A big deviation between the selected EAR and the minimum required EAR to avoid cavitation is noticed in the cupped propeller except in the higher sea states. Therefore, the probability of occurrence of cavitation is significantly reduced as the minimum required EAR to avoid cavitation is lower than the

selected EAR among most of the sea states; this difference between the two values increases while increasing the percentage of cupping shown in Figure 8b.



(a)

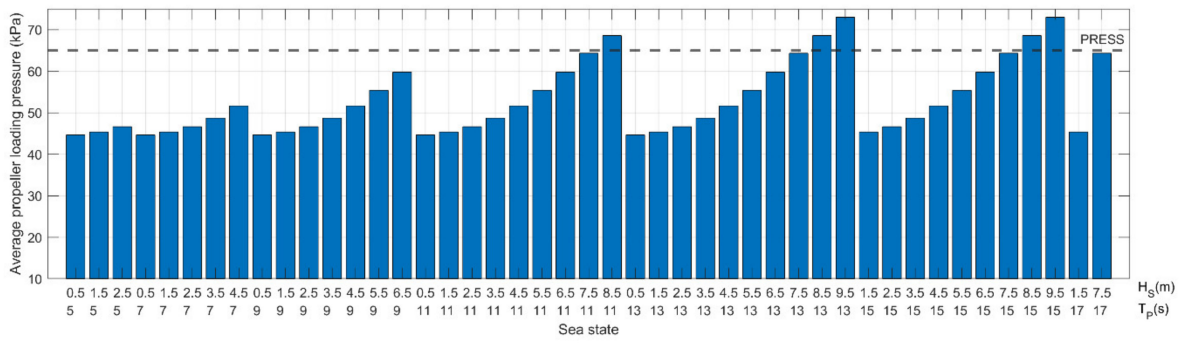


(b)

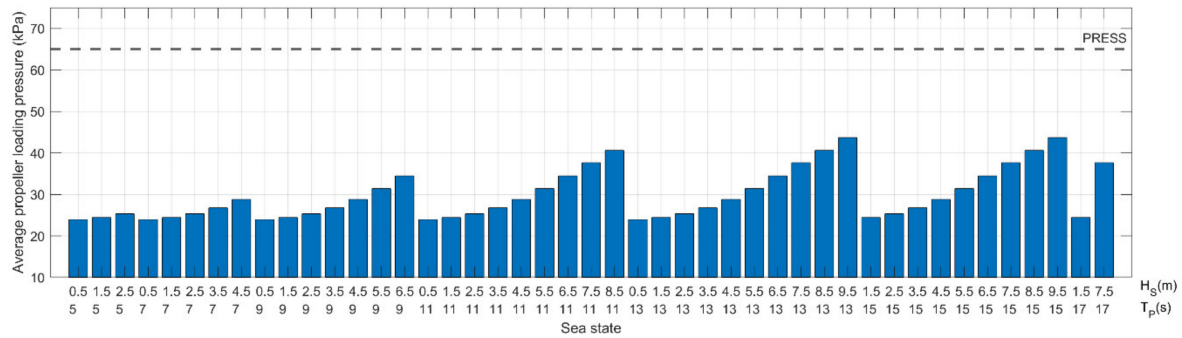
Figure 8. Variation of the minimum EAR for different sea states. (a) no cup, (b) heavy cup.

Based on the Burrill method, the average propeller loading pressure is computed and presented in Figure 9. Figure 9a shows the average propeller loading pressure for the uncupped propeller; it shows that the cavitation can occur at the higher sea state with more than 8.5 m significant wave height as the average propeller loading pressure values exceed the maximum limit required to avoid cavitation (65 kPa) suggested by HydroComp [40]; however, the values of the average propeller loading pressure decrease while increasing the cupping percentage. Thus, the occurrence of cavitation is significantly reduced among the sea states, as shown in Figure 9b.

The average predicted back cavitation percentage follows the same trend as the average propeller loading pressure. The cavitation can occur for uncupped propeller and in case of significant wave height with more than 8.5 m as the average predicted back cavitation percentage values exceed the 15% limit suggested by HydroComp [40] shown in Figure 10a. While increasing the cupping percentage, the average predicted back cavitation percentage values significantly decreased and reached their lowest level, as shown in Figure 10b.

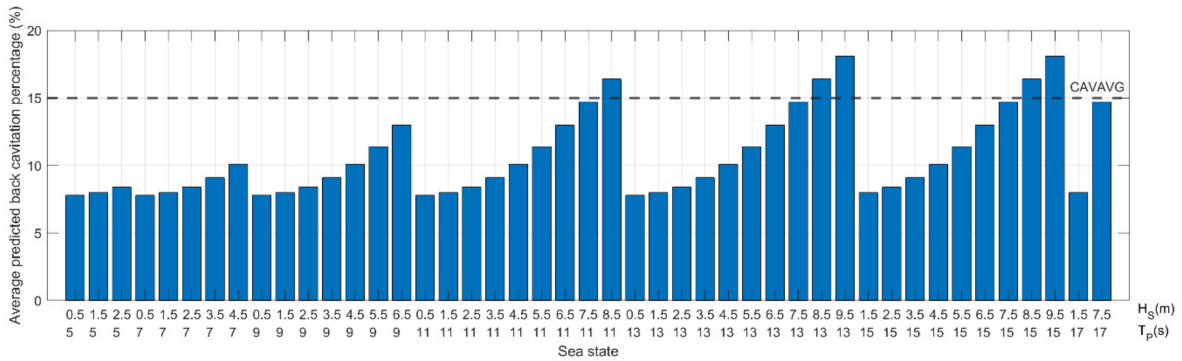


(a)

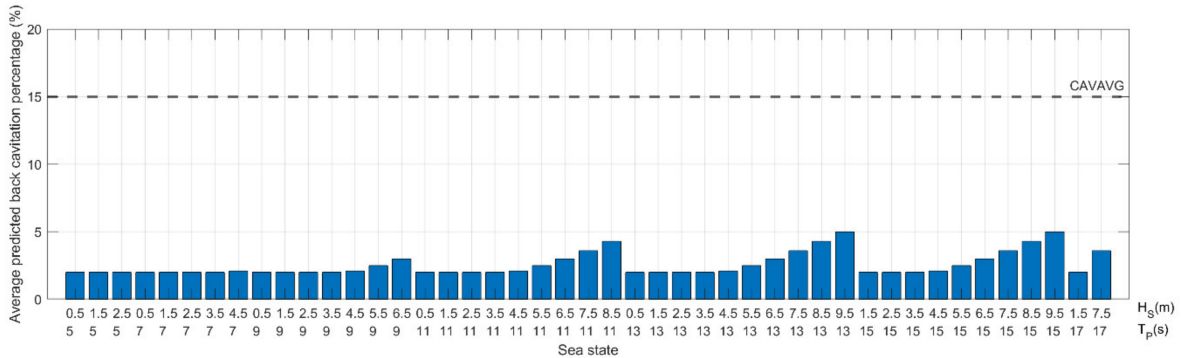


(b)

Figure 9. Variation of average propeller loading pressure for different sea states. (a) no cup, (b) heavy cup.



(a)



(b)

Figure 10. Variation of average back cavitation percentage for different sea states. (a) no cup, (b) heavy cup.

Regarding the noise level evaluated by the tip speed, all the optimized propellers, either with or without a cup, comply with the maximum noise level equal to 46 m/s and show the same trend, as shown in Figure 11.

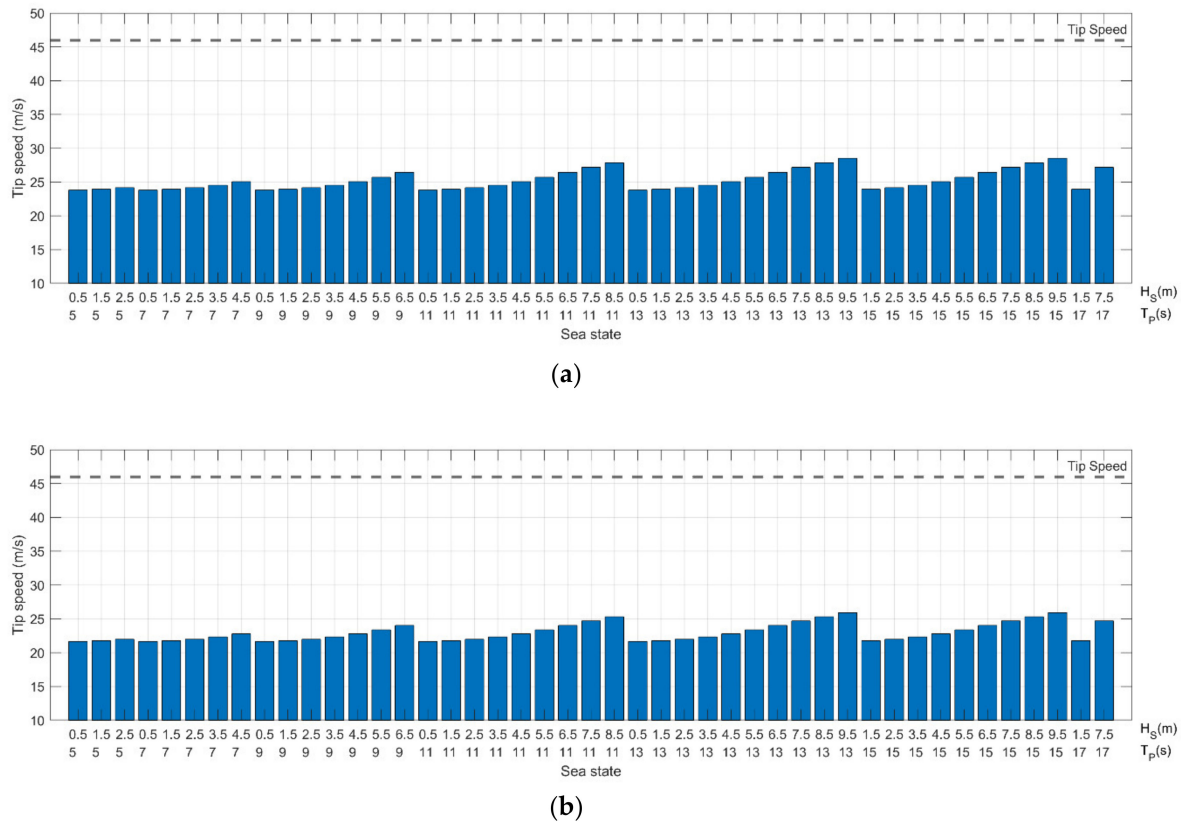
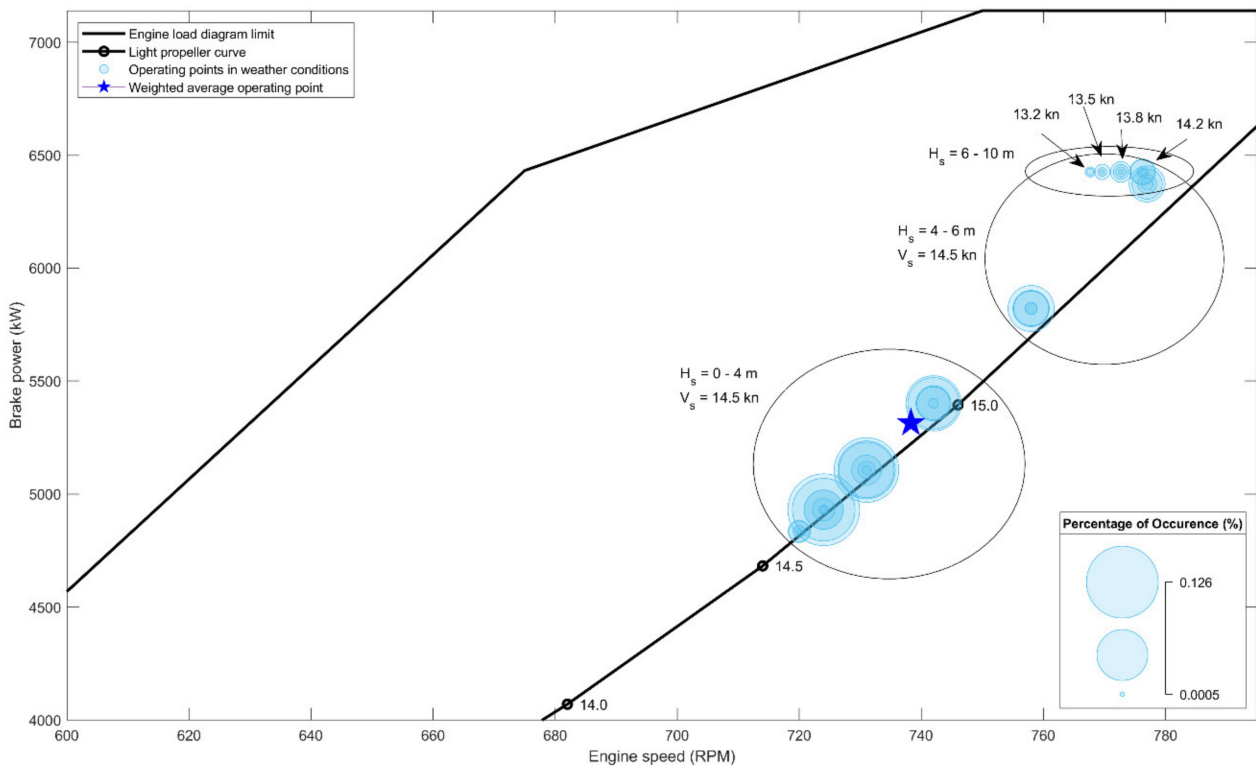


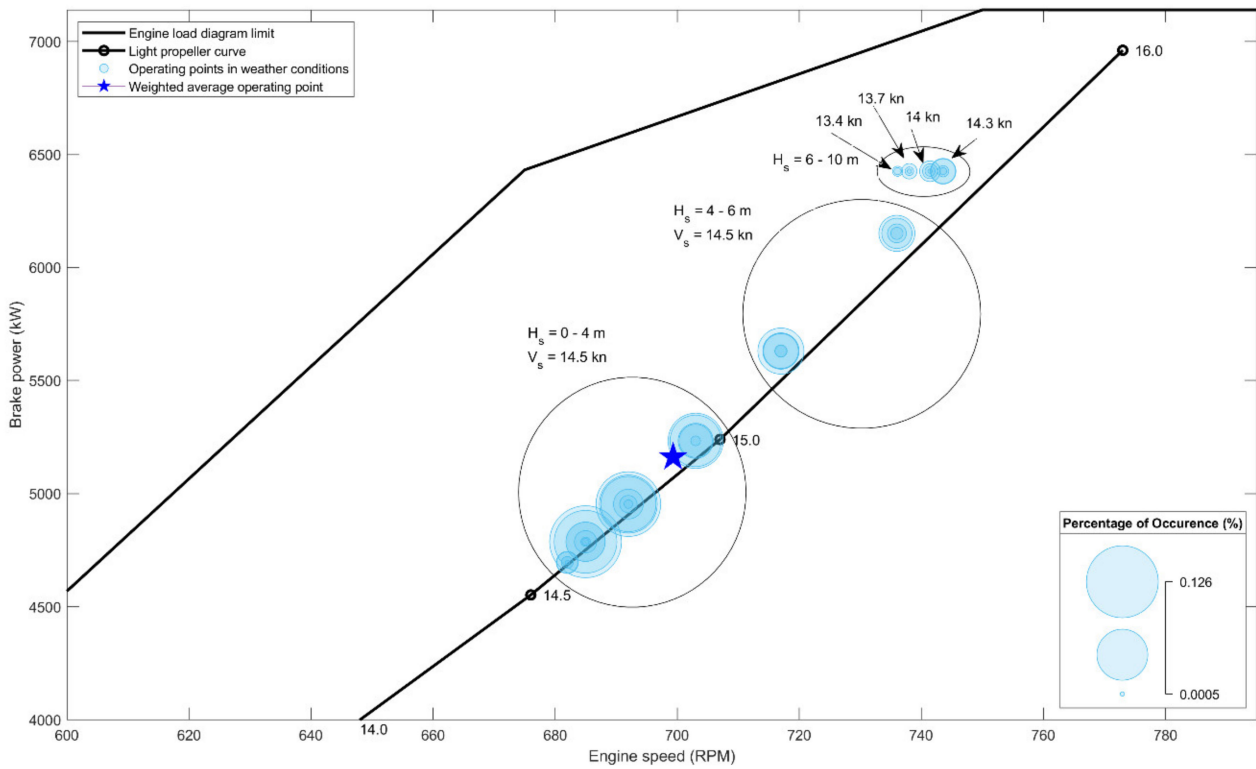
Figure 11. Variation of tip speed for different sea states. (a) no cup, (b) heavy cup.

Figure 12 shows the propeller performance inside the engine load diagram where no speed reduction is performed when the ship operates in sea states with a significant wave height below 6 m. With more than 6 m significant wave height, a reduction technique is considered to avoid the engine from overloading with no more than 90% of the rated power, where the brake power and engine speed are corrected and the reduction in ship speed is computed. By comparing the two sub-figures, there is no significant difference in speed reduction between the cases (up to 0.2 kn).

Finally, Table 4 presents the weighted average of the main important parameters based on the number of occurrences of each sea state to evaluate the effect of cupping percentage among the ship route; it has been found the weighted average engine speed is reduced while increasing the cupping percentage by 4.0%, 4.5% and 5.3% for light, medium and heavy cups, respectively. The weight average brake power is increased by 1% in the case of a light cup compared to no cup, following the same concept in calm water; however, the weight average brake power is reduced by 0.3% and 2.8% in the case of medium and heavy cups, respectively, compared to the uncapped propeller. The weighted average ship speed is almost the same among the four cases at around 14.47 kn.



(a)



(b)

Figure 12. Propeller performance inside engine load diagram. (a) no cup, (b) heavy cup.

Table 4. Comparison between the weighted average results of the simulated cases.

Item (Weighted Average)	Unit	No Cup	Light Cup	Medium Cup	Heavy Cup
Engine speed	rpm	738	708	705	699
Brake power	kW	5314	5370	5298	5161
Ship speed	Knot	14.47	14.47	14.47	14.48
Fuel consumption	l/nm	89.54	88.41	87.03	83.61

The weighted average fuel consumption is computed among the four cases, as the main parameter used to evaluate the propeller performance; it has been shown that the fuel consumption in the case of a light cup is reduced by 1.3% compared to the uncapped propeller; this percentage value is increased while considering the medium cup to achieve a fuel consumption reduction of 2.8%. The maximum reduction in fuel consumption is achieved by the propeller with a heavy cup with a 6.6% reduction compared to the case of the uncapped propeller.

4. Conclusions

This paper presents the effect of the propeller cup on propeller performance as a solution toward increasing the ship's energy efficiency by reducing the level of fuel consumption and thus reducing the level of emissions. Different cupping percentages are considered in this study, varying from no cup, passing through the light and medium cup to the heavy cup percentage. A propeller optimization model previously developed coupling NavCad and Matlab is used to perform the simulation using empirical formulas and optimize the geometry and operating point of the propeller for each cupping percentage. The main objective of this optimization model is to select the propeller at the minimum operating point with fuel consumption while complying with the cavitation and noise limits.

The propeller is first optimized at the ship design speed in calm water conditions; then, the propeller performance is evaluated among several sea state conditions based on the computed ship resistance. The added resistance due to wave is computed based on the known significant wave height and modal wave period as suggested by the Aertssen method. Next, a speed reduction technique is considered to ensure the propeller operation inside the engine load diagram. Any operation point exceeding 90% of rated power will be reduced to operate at the defined limit of the continuous engine operation area (90% of the rated power). Finally, a weighted average technique is used to evaluate the overall performance of the ship route.

In terms of cavitation, it has been found that the propeller can be able to avoid cavitation while increasing the cupping percentage in both calm water and weather conditions based on the evaluation criteria suggested by Keller and Burrill.

In terms of fuel consumption, a significant reduction in fuel consumption is achieved by up to 5.4% in calm water and by up to 6.6% among the ship route.

This work presents a preliminary estimation of propeller performance with cupping percentage in both calm water and weather conditions. Validation procedures using CFD methods can be considered for future work to estimate the propeller performance as well as the values of propulsive coefficients in different sea conditions.

Author Contributions: The concept of the problem is developed by M.T. The analysis is performed by M.T. and the writing of the original draft manuscript is done by M.T., R.V., M.V. and C.G.S. All authors have read and agreed to the published version of the manuscript.

Funding: This work was performed within the scope of the Strategic Research Plan of the Centre for Marine Technology and Ocean Engineering (CENTEC), which is financed by the Portuguese Foundation for Science and Technology (Fundação para a Ciência e Tecnologia-FCT) under contract UIDB/UIDP/00134/2020.

Institutional Review Board Statement: Not applicable.

Informed Consent Statement: Not applicable.

Data Availability Statement: The data presented in this study are available on request from the corresponding author.

Conflicts of Interest: The authors declare no conflict of interest.

References

- IMO-MEPC. Reduction of GHG emissions from ships. In *Fourth IMO GHG Study 2020*; IMO: London, UK, 2020; Volume 53, pp. 1689–1699.
- Green Ship of the Future. 2019 Retrofit Project. Available online: <https://greenship.org/project/2019-retrofit-series/> (accessed on 8 December 2021).
- Tadros, M.; Ventura, M.; Guedes Soares, C. Optimization procedure to minimize fuel consumption of a four-stroke marine turbocharged diesel engine. *Energy* **2019**, *168*, 897–908. [CrossRef]
- Korberg, A.D.; Brynolf, S.; Grahn, M.; Skov, I.R. Techno-economic assessment of advanced fuels and propulsion systems in future fossil-free ships. *Renew. Sustain. Energy Rev.* **2021**, *142*, 110861. [CrossRef]
- Chiong, M.-C.; Kang, H.-S.; Shaharuddin, N.M.R.; Mat, S.; Quen, L.K.; Ten, K.-H.; Ong, M.C. Challenges and opportunities of marine propulsion with alternative fuels. *Renew. Sustain. Energy Rev.* **2021**, *149*, 111397. [CrossRef]
- Altosole, M.; Benvenuto, G.; Campora, U.; Laviola, M.; Zaccone, R. Simulation and performance comparison between diesel and natural gas engines for marine applications. *Proc. Inst. Mech. Eng. Part M J. Eng. Marit. Environ.* **2017**, *231*, 690–704. [CrossRef]
- Tadros, M.; Ventura, M.; Guedes Soares, C. A Review of the Use of Biodiesel as a Green Fuel for Diesel Engines. In *Developments in Maritime Technology and Engineering*; Guedes Soares, C., Santos, T., Eds.; Taylor & Francis Group: London, UK, 2021; Volume 2, pp. 481–490.
- Elkafas, A.G.; Elgohary, M.M.; Shouman, M.R. Numerical analysis of economic and environmental benefits of marine fuel conversion from diesel oil to natural gas for container ships. *Environ. Sci. Pollut. Res.* **2021**, *28*, 15210–15222. [CrossRef]
- Wärtsilä. Wärtsilä Advances Carbon Capture and Storage in Maritime as Part of LINCCS Consortium. Available online: <https://www.wartsila.com/media/news/08-09-2021-wartsila-advances-carbon-capture-and-storage-in-maritime-as-part-of-linccs-consortium-2972116> (accessed on 10 January 2022).
- Irena, K.; Ernst, W.; Alexandros, C.G. The cost-effectiveness of CO₂ mitigation measures for the decarbonisation of shipping. The case study of a globally operating ship-management company. *J. Clean. Prod.* **2021**, *316*, 128094. [CrossRef]
- Ventura, M.; Guedes Soares, C. Integration of a Voyage Model Concept into a Ship Design Optimization Procedure. In *Towards Green Marine Technology and Transport*; Guedes Soares, C., Dejhalla, R., Pavletic, D., Eds.; Taylor & Francis Group: London, UK, 2015; pp. 539–548.
- Zha, L.; Zhu, R.; Hong, L.; Huang, S. Hull form optimization for reduced calm-water resistance and improved vertical motion performance in irregular head waves. *Ocean. Eng.* **2021**, *233*, 109208. [CrossRef]
- Feng, Y.; el Moctar, O.; Schellin, T.E. Parametric Hull Form Optimization of Containerships for Minimum Resistance in Calm Water and in Waves. *J. Mar. Sci. Appl.* **2021**, *20*, 670–693. [CrossRef]
- Farkas, A.; Degiuli, N.; Martić, I.; Dejhalla, R. Numerical and experimental assessment of nominal wake for a bulk carrier. *J. Mar. Sci. Technol.* **2019**, *24*, 1092–1104. [CrossRef]
- Ammar, N.R.; Seddiek, I.S. Wind assisted propulsion system onboard ships: Case study Flettner rotors. *Ships Offshore Struct.* **2021**, *1*, 1–12. [CrossRef]
- Lakshmi, E.; Priya, M.; Achari, V.S. An overview on the treatment of ballast water in ships. *Ocean Coast. Manag.* **2021**, *199*, 105296. [CrossRef]
- Lu, K.-T.; Lui, H.-K.; Chen, C.-T.A.; Liu, L.-L.; Yang, L.; Dong, C.-D.; Chen, C.-W. Using Onboard-Produced Drinking Water to Achieve Ballast-Free Management. *Sustainability* **2021**, *13*, 7648. [CrossRef]
- Vettor, R.; Guedes Soares, C. Development of a ship weather routing system. *Ocean Eng.* **2016**, *123*, 1–14. [CrossRef]
- Zaccone, R.; Ottaviani, E.; Figari, M.; Altosole, M. Ship voyage optimization for safe and energy-efficient navigation: A dynamic programming approach. *Ocean Eng.* **2018**, *153*, 215–224. [CrossRef]
- Prpić-Oršić, J.; Vettor, R.; Faltinsen, O.M.; Guedes Soares, C. The influence of route choice and operating conditions on fuel consumption and CO₂ emission of ships. *J. Mar. Sci. Technol.* **2016**, *21*, 434–457. [CrossRef]
- Vettor, R.; Tadros, M.; Ventura, M.; Guedes Soares, C. Route Planning of a Fishing Vessel in Coastal Waters with Fuel Consumption Restraint. In *Maritime Technology and Engineering 3*; Guedes Soares, C., Santos, T.A., Eds.; Taylor & Francis Group: London, UK, 2016; pp. 167–173.
- Tadros, M.; Vettor, R.; Ventura, M.; Guedes Soares, C. Effect of Different Speed Reduction Strategies on Ship Fuel Consumption in Realistic Weather Conditions. In *Trends in Maritime Technology and Engineering*; Guedes Soares, C., Santos, T.A., Eds.; Taylor & Francis Group: London, UK, 2022; Volume 1, pp. 553–561.
- Vinayak, P.P.; Prabu, C.S.K.; Vishwanath, N.; Prakash, S.O. Numerical simulation of ship navigation in rough seas based on ecmwf data. *Brodogradnja* **2021**, *72*, 19–58. [CrossRef]

24. Tadros, M.; Ventura, M.; Guedes Soares, C. Optimization Scheme for the Selection of the Propeller in Ship Concept Design. In *Progress in Maritime Technology and Engineering*; Guedes Soares, C., Santos, T.A., Eds.; Taylor & Francis Group: London, UK, 2018; pp. 233–239.
25. Vlašić, D.; Degiuli, N.; Farkas, A.; Martić, I. The preliminary design of a screw propeller by means of computational fluid dynamics. *Brodogradnja* **2018**, *69*, 129–147. [[CrossRef](#)]
26. Bacciaglia, A.; Ceruti, A.; Liverani, A. Controllable pitch propeller optimization through meta-heuristic algorithm. *Eng. Comput.* **2020**, *37*, 2257–2271. [[CrossRef](#)]
27. Ghaemi, M.H.; Zeraatgar, H. Analysis of hull, propeller and engine interactions in regular waves by a combination of experiment and simulation. *J. Mar. Sci. Technol.* **2021**, *26*, 257–272. [[CrossRef](#)]
28. Dai, K.; Li, Y.; Gong, J.; Fu, Z.; Li, A.; Zhang, D. Numerical study on propulsive factors in regular head and oblique waves. *Brodogradnja* **2022**, *73*, 37–56. [[CrossRef](#)]
29. Sun, Y.; Wu, T.; Su, Y.; Peng, H. Numerical prediction on vibration and noise reduction effects of propeller boss cap fins on a propulsion system. *Brodogradnja* **2020**, *71*, 1–18. [[CrossRef](#)]
30. Tadros, M.; Ventura, M.; Guedes Soares, C. Optimum Design of a Container Ship's Propeller from Wageningen B-Series at the Minimum BSFC. In *Sustainable Development and Innovations in Marine Technologies*; Georgiev, P., Guedes Soares, C., Eds.; Taylor & Francis Group: London, UK, 2020; pp. 269–274.
31. Tadros, M.; Vettor, R.; Ventura, M.; Guedes Soares, C. Coupled Engine-Propeller Selection Procedure to Minimize Fuel Consumption at a Specified Speed. *J. Mar. Sci. Eng.* **2021**, *9*, 59. [[CrossRef](#)]
32. Tillig, F.; Ringsberg, J.; Mao, W.; Ramne, B. A generic energy systems model for efficient ship design and operation. *Proc. Inst. Mech. Eng. Part M J. Eng. Marit. Environ.* **2017**, *231*, 649–666. [[CrossRef](#)]
33. Marques, C.H.; Belchior, C.R.P.; Caprace, J.D. Optimising the engine-propeller matching for a liquefied natural gas carrier under rough weather. *Appl. Energy* **2018**, *232*, 187–196. [[CrossRef](#)]
34. Tadros, M.; Ventura, M.; Guedes Soares, C. Design of Propeller Series Optimizing Fuel Consumption and Propeller Efficiency. *J. Mar. Sci. Eng.* **2021**, *9*, 1226. [[CrossRef](#)]
35. MacPherson, D.M. Small Propeller Cup: A Proposed Geometry Standard and a New Performance Model. In Proceedings of the 8th Propeller and Shafting Symposium, Virginia Beach, VA, USA, 23–24 September 1997.
36. Hwang, J.-L.; Tsai, J.-F.; Li, C.-Y. Cupped propeller test and analysis. *Ship Technol. Res.* **1995**, *42*, 186–192.
37. Tsai, J.-F. Study on the cavitation characteristics of cupped foils. *J. Mar. Sci. Technol.* **1997**, *2*, 123–134. [[CrossRef](#)]
38. Yari, E.; Moghadam, A.B. BEM applied to the cup effect on the partially submerged propeller performance prediction and ventilation pattern. *J. Mar. Eng. Technol.* **2020**, *21*, 159–177. [[CrossRef](#)]
39. Samsul, M.B. Blade Cup Method for Cavitation Reduction in Marine Propellers. *Pol. Marit. Res.* **2021**, *28*, 54–62. [[CrossRef](#)]
40. HydroComp. NavCad: Reliable and Confident Performance Prediction. Available online: <https://www.hydrocompinc.com/solutions/navcad/> (accessed on 30 January 2019).
41. Tadros, M.; Ventura, M.; Guedes Soares, C. Data Driven In-Cylinder Pressure Diagram Based Optimization Procedure. *J. Mar. Sci. Eng.* **2020**, *8*, 294. [[CrossRef](#)]
42. Tadros, M.; Ventura, M.; Guedes Soares, C. A nonlinear optimization tool to simulate a marine propulsion system for ship conceptual design. *Ocean Eng.* **2020**, *210*, 107417. [[CrossRef](#)]
43. Tadros, M.; Ventura, M.; Guedes Soares, C. Optimization of the performance of marine diesel engines to minimize the formation of SOx emissions. *J. Mar. Sci. Appl.* **2020**, *19*, 473–484. [[CrossRef](#)]
44. Tadros, M.; Ventura, M.; Guedes Soares, C. Simulation of the Performance of Marine Genset Based on Double-Wiebe Function. In *Sustainable Development and Innovations in Marine Technologies*; Georgiev, P., Guedes Soares, C., Eds.; Taylor & Francis Group: London, UK, 2020; pp. 292–299.
45. MAN Diesel & Turbo. Four-Stroke Project Guides. Available online: <https://www.man-es.com/marine/products/planning-tools-and-downloads/project-guides/four-stroke> (accessed on 22 July 2022).
46. Bentley. MAXSURF: Maximize Vessel Performance. Available online: <https://www.bentley.com/en/products/product-line/offshore-structural-analysis-software/maxsurf> (accessed on 4 April 2020).
47. Oosterveld, M.; Van Oossanen, P. Further Computer-Analyzed Data of the Wageningen B-Screw Series. *Int. Shipbuild. Prog.* **1975**, *22*, 251–262. [[CrossRef](#)]
48. Holtrop, J. A statistical re-analysis of resistance and propulsion data. *Int. Shipbuild. Prog.* **1984**, *31*, 272–276.
49. Holtrop, J. A Statistical Resistance Prediction Method With a Speed Dependent Form Factor. In Proceedings of the Scientific and Methodological Seminar on Ship Hydrodynamics (SMSSH '88), Varna, Bulgaria, 17–22 October 1988; Bulgarian Ship Hydrodynamics Centre: Varna, Bulgaria, 1988; pp. 1–7.
50. Holtrop, J.; Mennen, G.G.J. An approximate power prediction method. *Int. Shipbuild. Prog.* **1982**, *29*, 166–170. [[CrossRef](#)]
51. Islam, H.; Ventura, M.; Guedes Soares, C.; Tadros, M.; Abdelwahab, H.S. Comparison between Empirical and CFD Based Methods for Ship Resistance and Power Prediction. In *Trends in Maritime Technology and Engineering*; Guedes Soares, C., Santos, T.A., Eds.; Taylor & Francis Group: London, UK, 2022; Volume 1, pp. 347–357.
52. Tadros, M.; Ventura, M.; Guedes Soares, C. Surrogate Models of the Performance and Exhaust Emissions of Marine Diesel Engines for Ship Conceptual Design. In *Maritime Transportation and Harvesting of Sea Resources*; Guedes Soares, C., Teixeira, A.P., Eds.; Taylor & Francis Group: London, UK, 2018; pp. 105–112.

53. The MathWorks Inc. Fmincon. Available online: <https://www.mathworks.com/help/optim/ug/fmincon.html> (accessed on 2 June 2017).
54. Vettor, R.; Guedes Soares, C. Detection and Analysis of the Main Routes of Voluntary Observing Ships in the North Atlantic. *J. Navig.* **2015**, *68*, 397–410. [[CrossRef](#)]
55. Vettor, R.; Guedes Soares, C. Assessment of the storm avoidance effect on the wave climate along the main North Atlantic routes. *J. Navig.* **2016**, *69*, 127–144. [[CrossRef](#)]
56. Aertssen, G. The Effect of Weather on Two Classes of Container Ships in the North Atlantic. *Nav. Archit.* **1975**, *1*, 11–13.
57. Carlton, J. *Marine Propellers and Propulsion*, 2nd ed.; Butterworth-Heinemann: Oxford, UK, 2012.
58. Burrill, L.C.; Emerson, A. Propeller cavitation: Further tests on 16in. propeller models in the King's College cavitation tunnel. *Int. Shipbuild. Prog.* **1963**, *10*, 119–131. [[CrossRef](#)]
59. MacPherson, D.M. Reliable Propeller Selection for Work Boats and Pleasure Craft: Techniques Using a Personal Computer. In *Fourth Biennial Power Boat Symposium*; SNAME: Alexandria, VA, USA, 1991.
60. Saettone, S.; Taskar, B.; Steen, S.; Andersen, P. Experimental measurements of propulsive factors in following and head waves. *Appl. Ocean Res.* **2021**, *111*, 102639. [[CrossRef](#)]
61. Keller, W.H. Extended Diagrams for Determining the Resistance and Required Power for Single-Screw Ships. *Int. Shipbuild. Prog.* **1973**, *20*, 133–142. [[CrossRef](#)]